



## The effect of PDMS on Ti6Al4V for surface anti-wear and corrosion resistance

Mohd Harizan Zul <sup>1</sup>, Ramdziah Md Nasir <sup>2\*</sup>, Mahadzir Ishak <sup>1</sup>, Moinuddin Mohammed Quazi <sup>1</sup>

<sup>1</sup> Faculty of Mechanical and Automotive Engineering Technology, Universiti Malaysia Pahang Al-Sultan Abdullah, MALAYSIA.

<sup>2</sup> School of Mechanical Engineering, Universiti Sains Malaysia, MALAYSIA.

\*Corresponding author: ramdziah@usm.my

KEYWORDS	ABSTRACT
PDMS Ti6Al4V Laser texturing Frictional wear Corrosion	<p>This paper explores the effectiveness of Polydimethylsiloxane (PDMS) coating combined with laser texturing on Ti6Al4V surfaces to enhance wear and corrosion resistance for various industrial applications. The methodology involves initially applying PDMS coating on the sample surface, followed by laser texturing (PDMS-LT) to achieve superhydrophobic surface wetting behavior. The samples are subjected to wear sliding tests under dry, artificial seawater, and engine oil environments at a load of 10N and a speed of 75 m/min for 30 minutes, alongside corrosion potentiodynamic tests conducted in artificial seawater conditions. The results indicate a substantial improvement in wear resistance, specifically, the PDMS-LT demonstrated a notable 29.41% enhancement in wear resistance compared to untreated Ti6Al4V, exhibiting a wear rate of <math>3.45 \times 10^{-3} \text{ mm}^3/\text{m.N}</math>. Moreover, under oil lubrication conditions, PDMS-LT exhibited a significant reduction in wear rate, measuring at <math>2.83 \times 10^{-4} \text{ mm}^3/\text{m.N}</math>, representing an impressive 80% enhancement over untreated surfaces. The corrosion resistance is notably improved with PDMS-LT surface exhibits a significantly reduced corrosion rate by 84% compared to UT surface. In conclusion, the results emphasize the potential of PDMS superhydrophobic fabrication combined with laser texturing to enhance the durability and performance of Ti6Al4V components across diverse industrial applications.</p>

Received 22 July 2024; received in revised form 14 October 2024; accepted 22 November 2024.

To cite this article: Zul et al., (2024). The effect of PDMS on Ti6Al4V for surface anti-wear and corrosion resistance. Jurnal Tribologi 43, pp.138-157.

## 1.0 INTRODUCTION

Titanium alloy grade 5 (known as Ti6Al4V) is extensively used in many vital industries, like aerospace, automotive and marine because of its remarkable properties such as strength to weight ratio, light weight and biocompatibility, which make it vital for numerous components (Kumar & Singh 2024). However, Ti6Al4V also faces challenges such as failures caused by wear (Harun et al., 2020) and corrosion (Guan et al., 2021) raise concerns about the materials reliability and durability for industrial environments.

Hu & Xu (2016) define the frictional wear is the term which refers to the material gradually wearing down caused by the surface rubbing against one another. It is crucial to comprehend the complexities of wear especially considering the use of Ti6Al4V in various machinery and equipment sectors (Khatri et al., 2024). Resolving this issue is crucial to enhancing the lifetime and performance of components. Surface modification like laser texturing offer a way to enhance the materials ability to withstand wear by customizing its surface properties (Alsaigh, 2024).

Laser texturing (LT) is a method used in surface engineering, where laser energy is carefully applied to create micro/nanoscale surface changes. This process allows for the development of surface designs that can affect how friction works and improve resistance to wear (Cholkar et al., 2023). Lei et al. (2024) notably laser texturing has proven to boost the characteristics of Ti6Al4V surfaces by lowering friction levels and enhancing wear resistance. Laser texturing shows potential in improving corrosion resistance making the material more suitable, for demanding conditions (Madapana et al., 2024; Velayuthaperumal & Radhakrishnan, 2024).

The performance of Ti6Al4V components is largely dependent on surface wetting behavior, which is regulated by surface topography and chemistry. This is especially true in settings where exposure to liquids or moisture is common. Superhydrophobic surfaces, characterized by their ability to repel water, offer significant advantages in terms of reduced friction and enhanced corrosion resistance (Rasitha et al., 2024). According to L. Hu et al. (2018), Polydimethylsiloxane (PDMS) is a crucial medium for creating superhydrophobic surfaces on Ti6Al4V. The application of PDMS on the laser-textured surface significantly alters the surface chemistry and enhances its functional properties. PDMS is known for its excellent hydrophobic properties (Davaasuren et al., 2014; Kameya, 2017; Olkowicz et al., 2022), thermal stability (Sulym et al., 2024), and chemical inertness (Zhu et al., 2020). Based on research by Olkowicz et al. (2022) laser texturing produces a rough surface that, when paired with a PDMS coating, significantly reduces surface free energy, yielding an average contact angle up to 159°. Davaasuren et al. (2014) found that a maximum water droplet contact angle of 171° was successfully achieved by fabricating a superhydrophobic surface on PDMS material also using the laser texturing of grid patterning. Based on the study by Kameya (2017), PDMS material with micropillar arrays reach 140° have potential uses in many fields, including microfluidics technologies.

Despite PDMS-based superhydrophobic surfaces being effective in various applications, further research is needed to understand their behavior in environments which undergo mechanical interactions and exposure to corrosive substances. This study aims to investigate how PDMS coating and laser texturing improve wear and corrosion resistance on Ti6Al4V surfaces. The objectives include creating superhydrophobic surfaces through these techniques, characterizing them through extensive studies, and examining their impact on frictional and anti-wear properties, as well as improving the corrosion resistance, which ultimately aiming to enhance Ti6Al4V performance in industrial settings.

## 2.0 EXPERIMENTAL PROCEDURE

### 2.1 Materials and Preparation

Ti6Al4V samples (from Nippon Steel) are prepared for experimentation. These samples, cut to size of 65mm x 15mm with a thickness of 1.2mm, will go through rigorous surface preparation to ensure uniformity and cleanliness. Initially, the samples are subjected to a series of polishing steps using SiC grit abrasive papers with grit sizes of 240, 400, 800, and 1200. This process aims to remove surface flaws and provide a mirror-like finish. After polishing, the samples are completely cleaned using an ultrasonic bath in an acetone solution for 10 minutes. The samples are then allowed to naturally air dry to avoid contamination.

### 2.2 Surface Fabrication

Superhydrophobic surfaces on Ti6Al4V are created via a two-step process that starts with polydimethylsiloxane (PDMS) coating by applying a stroke brush on the sample and then followed by laser texturing (label as PDMS-LT) as shown in Figure 1. The PDMS coating is performed with a previously established silanization hybrid method by Zul et al. (2023). The laser parameters were set to create a texture on the surface are shown in Table 1. The sample laser texture which was not coated with PDMS was labeled as LT.

Table 1: The laser texturing parameters.

Laser parameter	Unit	Value
Power	Watt, W	18
Speed	mm/s	220
Frequency	KHz	40
Environment		Argon flow
Pattern		Grid
Distances between hatches	mm	0.45

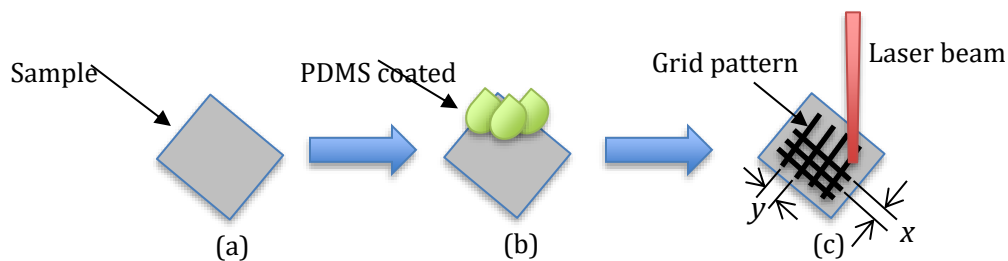


Figure 1: The surface fabrication of PDMS prior to laser texturing. (a) untextured surface (UT), (b) PDMS coating, (c) PDMS-Laser texturing (PDMS-LT). Distances between hatches is noted by  $x=y=0.5\text{mm}$ .

### 2.3 Wettability Test

The wettability test procedure began by cleaning the laser-textured samples in an ultrasonic bath with acetone, followed by natural air drying. Once dried, the sample was placed on the stage of a contact angle (CA) tester (LR-SDC-100, Changsha Lonroy Technology Co. Ltd, China). The test began immediately after the sample are dried. A 20  $\mu\text{L}$  droplet of deionized water was dispensed

onto the sample for contact angle measurement. The readings were taken from five different spots on the sample. Images of the water droplets were captured and analyzed using CA software, which automatically provided the contact angle results.

## 2.4 Surface Characteristics Analysis

A comprehensive analysis of the surface characteristics of the fabricated samples is conducted to elucidate the effects of the PDMS coating and laser texturing. Surface topography is examined using a state-of-the-art 3D laser microscope (Olympus LEXT OLS5000 series) to visualize surface profile and roughness. Additionally, surface composition elemental analysis is performed utilizing a scanning electron microscope coupled with energy-dispersive X-ray spectroscopy (SEM-EDX), specifically the JEOL JSM-IT 200 model.

Surface microhardness, an indicator of material strength, is measured using a Vickers hardness tester (FV-310, Future Tech) to assess the impact of surface modification on mechanical properties. Figure 2 shows the cross-sectional area with the location of 15 indentation point after PDMS coated with laser textured surface.

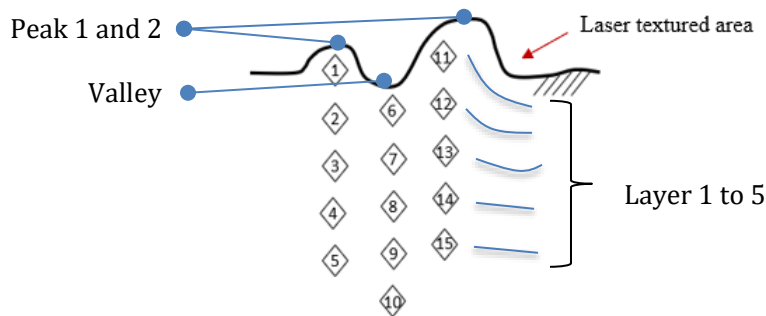


Figure 2: Indentation location under laser textured surface.

## 2.5 Wear Sliding Test

The wear behavior of the samples is evaluated through wear sliding tests conducted using a Ducom TR-20 ball-on-flat tribometer. A  $\text{Si}_3\text{N}_4$  ball with a 10mm diameter serves as the counter face. The test parameters of sliding wear experiment according to the ASTM G133-05(2016) standard, including load (10N), sliding speed (75m/min), and duration (1800s) (Xu et al., 2021). Tests are conducted under dry, artificial seawater (SW), and oil lubrication conditions to assess the samples' performance in different environments. Wear rates, WR are quantified by measuring weight loss using a Shimadzu (AUW220D) digital electronic balancer, while coefficient of friction (COF) is continuously monitored throughout the test using Winducom 2010 software.

## 2.6 Corrosion Behavior Analysis

Corrosion behavior is evaluated using a Gamry Interface1000E potentiostat/galvanostat corrosion workstation. Potentiodynamic polarization tests are performed at standard room temperature in an artificial seawater medium to simulate corrosive conditions. A standard three-electrode system is employed, comprising the working electrode (samples), counter electrode (graphite), and reference electrode (silver chloride). Corrosion potential and current density are analyzed using Tafel-type fit analysis software to ascertain the corrosion resistance of the modified surfaces.

### 3.0 RESULTS AND DISCUSSION

#### 3.1 Surface Characteristics

##### 3.1.1 Surface Topography

After laser texturing of Ti6Al4V, the sample with grid pattern was subjected to surface topographical analysis using a 3D laser microscope. The results are summarized in Figure 3, and the following analysis and discussion highlight the significant findings and comparisons among the different patterns.

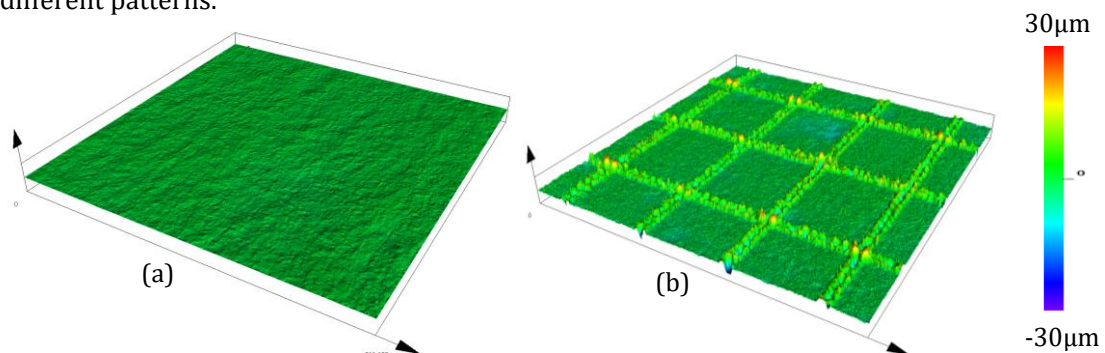


Figure 3: Surface of (a) raw surface (untextured) and (b) after laser texturing with grid-array pattern.

Surface roughness and pattern morphology are crucial features that can be described by various surface roughness parameters according to the national standard ISO25187 (Tan et al., 2021). These parameters encompass both two-dimensional and three-dimensional roughness metrics. Among the common parameters, the average roughness ( $S_a$ ) provides a measure of the changes in the height of the surface datum but lacks sensitivity to small height changes and does not capture waveform information. The root means square roughness ( $S_q$ ), while more responsive to microscopic roughness changes compared to  $S_a$ , still falls short in adequately describing the three-dimensional characteristics of a rough surface (H. Yang et al., 2024). To address non-Gaussian distributions, amplitude parameters such as skewness ( $S_{sk}$ ) and kurtosis ( $S_{ku}$ ) are utilized.  $S_{sk}$  indicates the skewness of the rough surface, with zero skewness representing uniform distribution of peaks and pits, positive skewness indicating a high surface or fewer potholes, and negative skewness signifying deep scratches or lower peaks.  $S_{ku}$ , on the other hand, describes the sharpness of the surface peaks, where values less than 3 suggest shallower/broader peaks than a normal distribution, and values greater than 3 indicate sharper peaks.

The surface topographical analysis of laser-textured Ti6Al4V reveals significant variations in their roughness and texture characteristics, which are crucial for determining their functional properties. Figure 4 shows the surface areal roughness of untextured (UT), laser textured (LT) and laser textured prior to PDMS coating (PDMS-LT). The  $S_a$  and  $S_q$  measurements notably rise from the UT to LT and PDMS-LT surfaces suggesting that laser texturing and PDMS coating bring about roughness over the surface. This increased roughness can enhance the wettability characteristics of the surfaces.

In terms of the skewness (Ssk), the UT sample shows a value pointing towards more valleys compared to the LT and PDMS-LT surfaces that have positive skewness values suggestive of more peaks present, on them. This implies that laser texturing results in surfaces with peaks dominating them; however, applying a PDMS coating helps in smoothing out these peaks slightly reducing by 77% from LT to PDMS-LT. This smoothing effect could potentially lead to a distribution of forces during frictional contact which in turn might help reduce wear and tear.

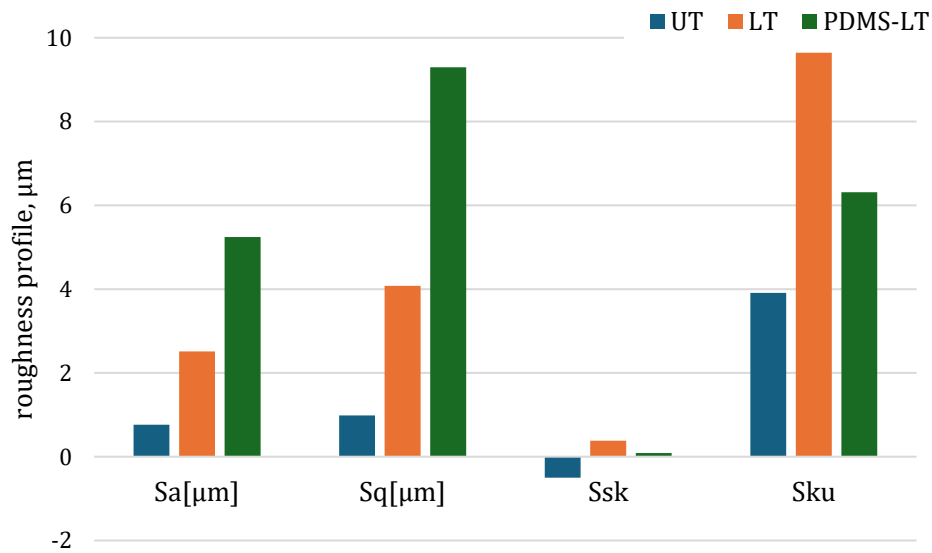


Figure 4: The results of surface roughness profile of untextured (UT) and laser-textured (UT) surfaces.

The Kurtosis (Sku) values reinforce these discoveries effectively; the UT surface exhibits a moderate peak sharpness whereas the LT surface displays a 53% significantly higher suggesting that the laser texturing brings about sharper peaks. Trying out a PDMS coating causes the kurtosis to drop implying that the coating smoothens some of these features resulting in an acute and extreme surface. The PDMS layers decrease, in kurtosis can enhance hydrophobicity by creating surfaces that are less sharp and more stable in forming liquid films which ultimately improves the water-resistant characteristics.

### 3.1.2 Surface Morphology

The elemental composition of the untextured, laser textured and the laser-textured surface coated bit PDMS (PDMS-LT) is significantly different at each stage of treatment as shown in Figure 5. The raw Ti6Al4V surface is primarily composed of titanium, aluminium, and vanadium, with small quantities of oxygen and carbon. This composition reflects the typical elemental makeup of Ti6Al4V alloy, indicating that the surface is clean and untreated. The surface elements composition changes significantly after laser texturing. The amounts of aluminium and vanadium slightly decrease, while the titanium content rises. Notably, there is an increase in carbon and oxygen content. According to Parmar et al. (2018) and Y. Wang et al. (2020), these alterations might be the result of carbonization or oxidation brought on by the laser texturing process, which

increases surface roughness and creates reactive sites. The increase in oxygen content indicates the formation of titanium oxides, which contribute to the altered surface properties (Huerta-Murillo et al., 2019).

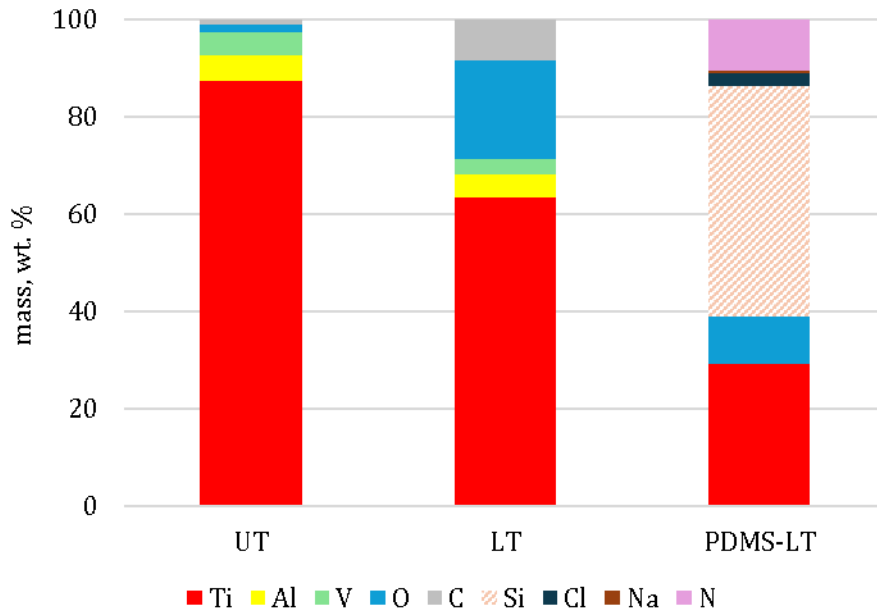


Figure 5: The results of SEM-EDX for raw surface, laser texture surface and laser textured after PDMS coated.

There are further notable modifications to the elemental composition when the PDMS coating is placed to the laser-textured surface. Additionally, the titanium concentration drops significantly, suggesting that the PDMS layer has covered a sizable portion of the surface. The PDMS covering is predominantly composed of silicon-based compounds, as shown by the presence of silicon (Si). The oxygen content is reduced by reflecting the partial coverage of oxides by the PDMS layer. The PDMS creates a strong layer over the laser-textured surface, shielding the underlying titanium alloy from more oxidation and wear, as shown by the significant drop in titanium content and the appearance of silicon.

The transition from a raw surface to a laser-textured one introduces more reactive sites and increases the surface roughness, which is beneficial for certain applications such as enhanced adhesion or wettability. However, the laser-textured surface, despite its increased functionality, is prone to oxidation and other environmental effects. The subsequent application of PDMS mitigates these issues by providing a hydrophobic barrier that repels water, reduces friction, and enhances the overall durability of the surface.

### 3.1.3 Surface microhardness

The results of the microhardness (Figure 6) indicate the noteworthy variations and offering information about how laser texturing affects the mechanical characteristics of the material. By measuring the hardness at different distance can determine how far away a hardness value from

its material surface. The microhardness of untextured surface is comparatively constant between at each distance. This consistency points to a homogeneous hardness profile in the raw material, which is typical of untreated Ti6Al4V.

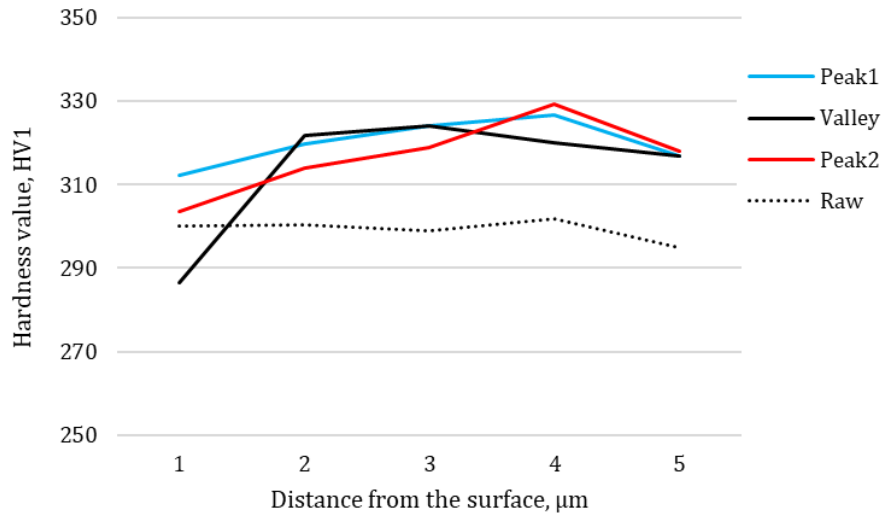


Figure 6: The results of microhardness for raw materials and laser textured surface.

The results show a distinct hardness profile for the laser-textured surface, with valleys found between two peaks. Peak 1 and Peak 2 have a different microhardness value but in a similar form while the hardness of valleys is the lowest near the surface but higher inside the material. The localized impacts of laser texturing are highlighted by the difference in hardness between peaks and valleys (Farrokhi et al., 2015). The peaks, which are the highest points of the laser-textured surface, generally exhibit higher hardness values compared to the valleys (Chauhan et al., 2021). The quick cooling and solidification that occurs during the laser texturing process is what causes the increase in hardness at the peaks. This improved microstructure and possible development of tougher phases are the results of this process (Chauhan et al., 2021).

The main findings indicate that laser texturing significantly modifies the surface hardness profile of Ti6Al4V. The enhanced hardness at the peaks suggests improved wear resistance, which is beneficial for applications requiring durable surfaces. The presence of valleys, although slightly lower in hardness, indicates a more complex topography that can enhance certain surface interactions (Trinh et al., 2017), such as improved adhesion or friction control. Compared to the untextured surface, the laser-textured surface exhibits higher and more variable hardness values. The UT consistent hardness reflects its uniform microstructure, whereas the laser-textured surface shows localized hardening effects due to the texturing process. This differentiation is crucial for applications where surface hardness and topographical features play a critical role in performance.

### 3.2 Effect of PDMS on Wetting Behaviour

Figure 7 displays the results of the water contact angle (WCA) measurements demonstrate the impact of PDMS coating on surface hydrophobicity. The untextured surface shows a WCA of 78°,



indicating low hydrophobicity (hydrophilic). Laser texturing with grid-array pattern increases the WCA to 98° (hydrophobic), showing improved water repellency due to the increased surface roughness. However, the most significant change occurs after the PDMS coating is applied to the laser-textured surface with similar pattern, with the WCA reaching 152° (superhydrophobic), signifying the creation of a superhydrophobic surface with excellent water-repellent properties.

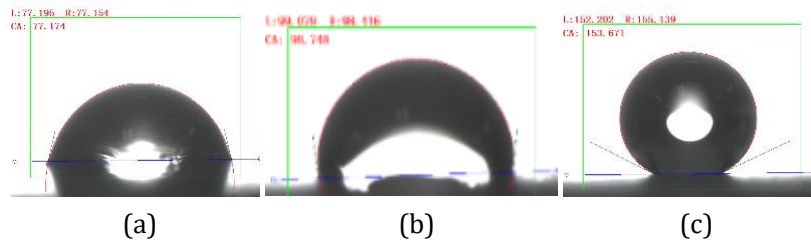


Figure 7: The results of water contact angle measurement of (a) untextured surface (UT), (b) laser textured surface (LT), and (c) laser textured surface prior to PDMS coating (PDMS-LT).

The increase in water contact angle (WCA) from 78° on the untextured (UT) surface to 98° on the laser-textured (LT) surface highlights the significant impact of surface roughness on hydrophobicity. Laser texturing creates microscale surface roughness, which traps air and reduces the contact area between water droplets and the surface. This results in a higher WCA, as rougher surfaces tend to repel water more effectively by decreasing surface energy and promoting water droplet beading, improving hydrophobic performance.

The application of PDMS further enhances surface hydrophobicity, rapidly transforming the laser-textured surface into a superhydrophobic one, increasing the WCA to 152°. PDMS, a hydrophobic polymer, significantly lowers the surface energy and accelerates the development of superhydrophobicity by coating the micro-roughness created by laser texturing. This combination of texture and low surface energy promotes the Cassie-Baxter wetting state, where water droplets sit on top of the surface without penetrating the micro-rough features, leading to faster and more effective water repellency.

### 3.2.1 Chemical Reaction of PDMS

A complex chemical transformation procedure is required to convert hydroxyl (-OH) groups on materials such as laser-textured Ti6Al4V to generate superhydrophobicity. After laser texturing, the Ti6Al4V surface is first exposed to air and moisture. (Yusuf et al., 2022) explain this phenomenon occurred from the water molecules adsorb onto the surface and forms hydroxyl groups (-OH) through a reaction between titanium atoms and water that produces Ti-OH and hydrogen gas, as shown in Equation (1) by He et al. (2020). These hydroxyl groups are hydrophilic, increasing the surface energy of the material.



To achieve superhydrophobicity, a chemical functionalization process called silanization is employed. In this process, the hydroxyl groups on the surface react with silane compounds forming a self-assembled monolayer of silane molecules. Z. Yang et al. (2018) explain that the

reaction replaces the hydrophilic -OH groups with hydrophobic alkyl chains, significantly lowering the surface energy. The chemical reaction can be represented as following Equation (2):



where, X represents a hydrophobic alkyl chain.

This transformation results in the creation of a hydrophobic coating on the Ti6Al4V surface. The lower surface energy, due to the presence of hydrophobic alkyl chains, enhances water repellency, causing water droplets to bead up and roll off the surface rather than spreading out (Schnell et al., 2020). The chemical bonds formed during silanization are typically stable, ensuring that the superhydrophobic properties are maintained over time (He et al., 2022). This entire process effectively converts the hydroxyl groups to hydrophobic groups, thus achieving and sustaining superhydrophobicity on the laser-textured Ti6Al4V surfaces (Guo & Zhao, 2024).

### 3.3 Surface Wear Performance

#### 3.3.1 Effect of Lubrication

The wear rate of untextured (UT), laser-textured (LT), and laser-textured with PDMS coating (PDMS-LT) surfaces of Ti6Al4V was investigated under three different environments: dry, seawater (SW), and oil lubrication as shown in Figure 8. In dry conditions, both the UT and LT surfaces exhibited identical wear rates, indicating that the laser texturing alone did not significantly improve the wear performance. However, the PDMS-LT surface showed a markedly reduced wear rate by 29.41% enhancement compared to UT ( $\text{WR } 3.45 \times 10^{-3} \text{ mm}^3/\text{m.N}$ ), which demonstrates the effectiveness of the PDMS coating in lowering wear rate. Similar results are also reported by Kumar et. al (2024) that the coatings can lower wear rates on Ti6Al4V alloys by enhancing surface properties.

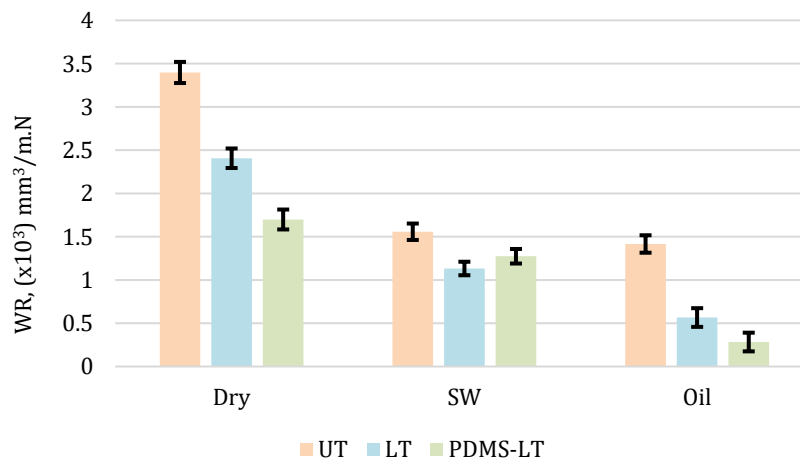


Figure 8: The wear rate for UT, LT, and PDMS-LT under different sliding mediums.

Under artificial seawater (SW), the wear rates for all surfaces decreased compared to dry conditions. The UT surface had a 54% lower wear rate compared the UT in dry condition, while the LT surface exhibited a further reduced wear rate, highlighting the positive impact of laser texturing in reducing wear when exposed to seawater. The PDMS-LT surface maintained a low wear rate, although slightly higher than the LT surface, indicating that while PDMS contributes to wear reduction, its effectiveness in seawater may be influenced by the interaction with the lubricant.

The most significant reduction in wear rates was observed under oil lubrication. The UT surface had a small improvement of wear rate than in seawater conditions. The LT surface showed a greater reduction of WR, underscoring the beneficial effects of laser texturing in the presence of oil. The PDMS-LT surface exhibited the lowest wear rate, measuring at  $2.83 \times 10^{-4} \text{ mm}^3/\text{m.N}$ , with an exceptionally 80% improvement over UT, demonstrating that PDMS coating significantly reduces wear rates in both seawater and oily conditions, consistent with He et al. (2020), which emphasized the role of hydrophobic coatings in wear reduction.

The study also found that the width of wear varied significantly under different environmental conditions as shown in Figure 9. The study reveals that the wear track width significantly decreases in lubricated environments compared to dry conditions, with the widest track observed in the dry environment, followed by seawater, and the narrowest in oil condition. This indicates that lubrication markedly reduces wear, with oil being more effective than seawater (Chauhan et al., 2021). The findings emphasize the importance of proper lubrication to enhance wear resistance and extend the lifespan of Ti6Al4V components (Nazrin et al., 2024). Additionally, the improved lubrication effectiveness may be influenced by the increased surface roughness from laser texturing.

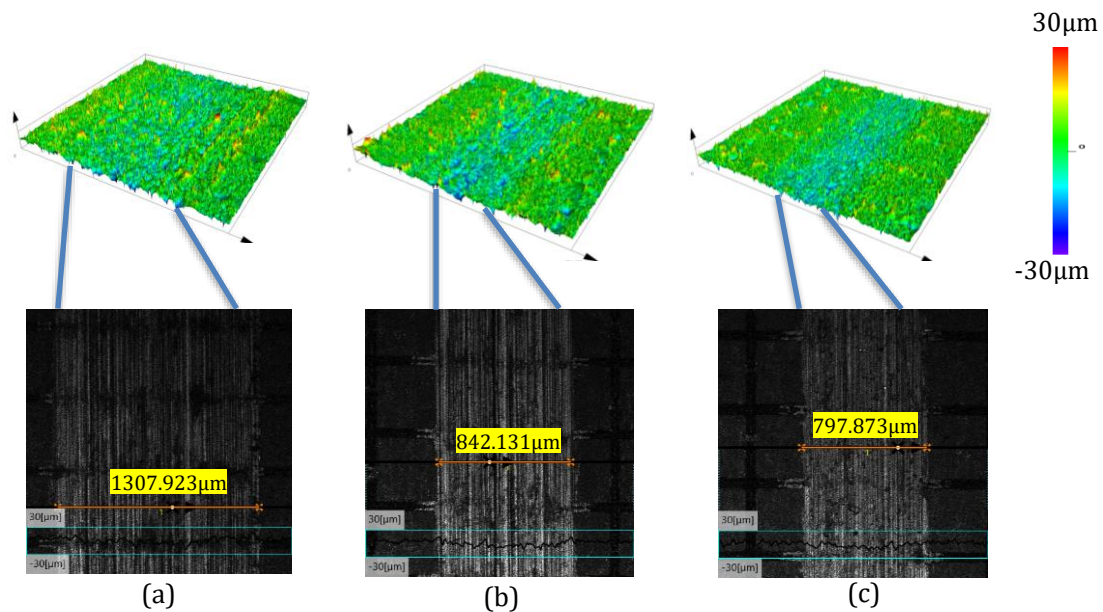


Figure 9: The width of wear track of laser textured surfaces under (a) dry, (b) seawater, and (c) oil conditions.

The surface profile of the laser-textured surfaces, characterized by valleys between peaks, significantly influence wear performance. These features trap wear debris and reduce abrasive wear (He et al., 2022). Additionally, Velayuthaperumal & Radhakrishnan (2024) reported that the valleys serve as micro-reservoirs for lubricants to enhance the lubrication under conditions like seawater and oil. This complex topography leads to lower wear rates for LT and PDMS-LT surfaces compared to UT surfaces. The improved lubrication and reduced wear in LT and PDMS-LT surfaces underscore the role of surface topography in enhancing wear resistance.

### 3.3.2 Effect Surface Topography

Surface roughness plays a critical role in wear performance (Z. Wang et al., 2022) as shown in Figure 10. The increased roughness of the LT surfaces compared to UT surfaces results in a higher initial contact area and more pronounced interactions with the counter face. The figure illustrates the effect of surface topography (Sa and Sq) on wear performance (WR). As surface roughness increases from UT to LT and PDMS-LT, there is a corresponding rise in wear rate. The PDMS-LT surface, with the highest Sa and Sq values, shows a higher wear rate (WR), indicating that excessive roughness may lead to increased wear. In contrast, LT shows a moderate roughness profile and a lower wear rate than PDMS-LT, suggesting that an optimal roughness improves wear resistance, while excessively rough surfaces may exacerbate wear.

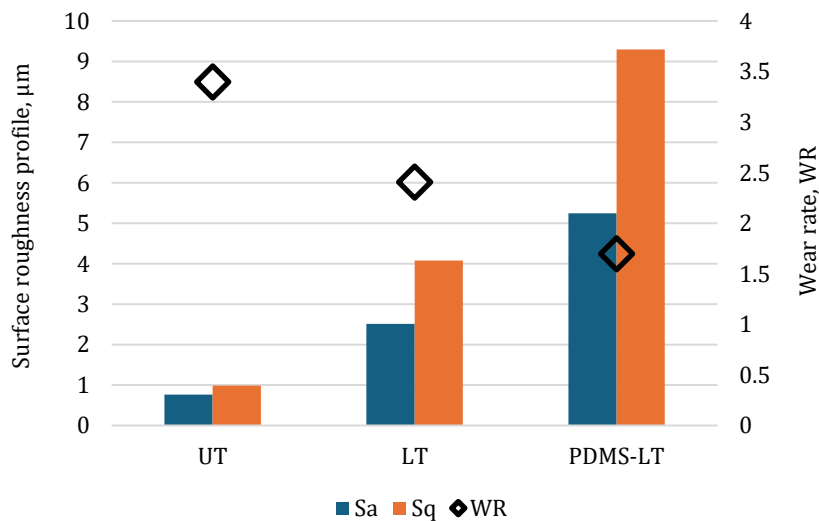


Figure 10: The relationship between wear rate and surface roughness for UT, LT and PDMS-LT.

### 3.3.3 Effect Surface Morphology

Figure 11 displays the result of SEM-EDX of the laser-textured (LT) surface before and after the wear test (LT-W). There is a significant increase in the titanium (Ti) content from 34%, while carbon (C) and oxygen (O) drop considerably after the wear test (from 67% and 86%, respectively). This can be attributed to the removal of oxidized layers and contamination on the surface due to the mechanical wear process. The sliding wear likely eroded the outer oxide and carbon-rich layers that had formed during laser texturing, exposing the underlying Ti substrate,

which results in an increase in the Ti signal detected by EDX. The decrease in oxygen and carbon is that the surface oxidation layer and organic contaminants were worn away during the test.

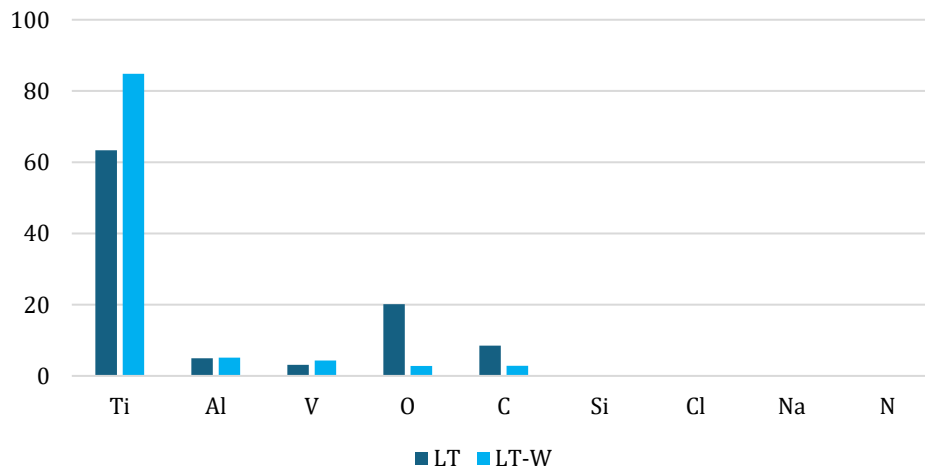


Figure 11: The result of SEM-EDX for LT and LT after wear sliding test.

For the PDMS-coated laser-textured surface (PDMS-LT) compared to after the wear test (PDMS-LT-W), titanium (Ti) shows a slight increase, while silicon (Si) decreases sharply by 97% as shown in Figure 12. Meanwhile, carbon (C) and oxygen (O) rise significantly after the wear test (C from 9.76% to 32.15%, O from 9.76% to 27.88%). This indicates that the PDMS coating, which contains a high concentration of silicon, was worn away during the wear test, thus reducing the Si content on the surface. The increase in carbon and oxygen suggests that some parts of the PDMS coating remained or became redistributed across the surface after wear, and oxidation likely occurred, leading to a higher oxygen content. The slight increase in titanium (Ti) after wear can be attributed to the exposure of the underlying Ti6Al4V alloy surface as the PDMS coating was gradually worn down.

In both cases, the wear test caused significant surface changes, exposing more of the underlying Ti in both LT and PDMS-LT samples. The reduction of carbon and oxygen in the LT sample suggests the removal of surface oxidation, while the PDMS-LT sample exhibited a marked reduction in silicon, indicating the wear of the PDMS layer. These changes provide insight into the wear behavior of laser-textured and PDMS-coated surfaces under sliding conditions, highlighting the role of surface layers in wear resistance.

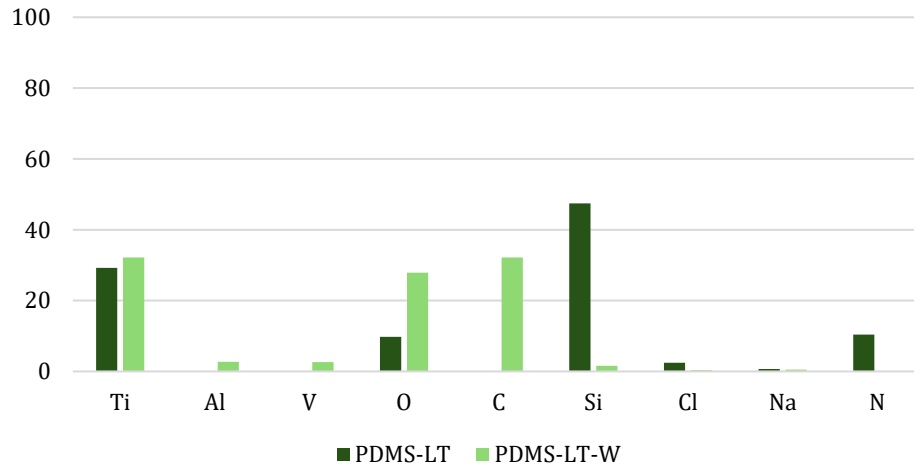


Figure 12: The result of SEM-EDX for PDMS coating sample before (PDMS-LT) and after wear sliding test (PDMS-LT-W).

### 3.3.3 Effect Surface Microhardness

The enhancement of microhardness through laser texturing significantly improves both wear resistance and the coefficient of friction (Figure 13) of Ti6Al4V surfaces. The increased hardness at the peaks of the textured surface reduces plastic deformation and wear during sliding, especially under lubricated conditions (Chauhan et al., 2021). This heightened hardness leads to lower COF values as the surface deforms less and maintains a consistent profile, thereby reducing frictional forces. Additionally, the PDMS coating further decreases wear rates and COF due to its low friction. Furthermore, PDMS-coated LT surfaces exhibit even lower wear rates, indicating that the coating, combined with the enhanced hardness from laser texturing, provides superior wear resistance. These results underscore the importance of surface hardening through laser texturing in enhancing the wear performance of Ti6Al4V.

The coefficient of friction (CoF) results also shows a clear relationship with surface microhardness, particularly after laser texturing and PDMS coating. Based in Figure 6, the microhardness values of laser-textured surfaces (Peaks 1 and 2) are significantly higher than the raw surface. This increased hardness reduces plastic deformation during sliding, helping to stabilize CoF, as shown in the PDMS-LT surface in Figure 13, which maintains the lowest and most stable CoF. The raw surface, with lower hardness, shows higher CoF, indicating that lower hardness contributes to higher friction and wear.

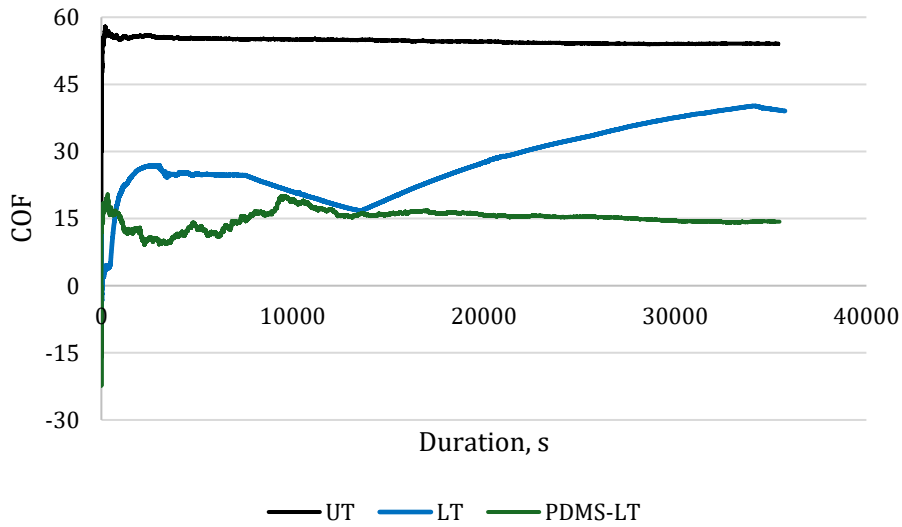


Figure 13: COF for UT, LT and PDMS-LT.

### 3.4 Corrosion Properties

Figure 14 illustrates the corrosion resistance for untextured (UT), laser-textured (LT), and PDMS-coated laser-textured (PDMS-LT) Ti6Al4V. The lowest corrosion rate is shown by the untextured (UT) surface. The corrosion rate is considerably decreased via laser texturing (LT). This improvement in corrosion resistance can be linked to surface morphological changes and the formation of a more passive oxide layer.

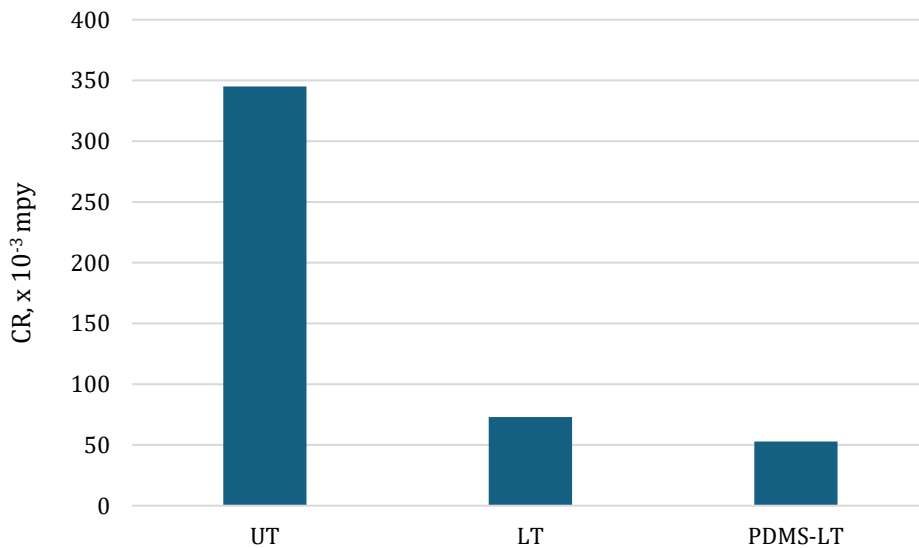


Figure 14: Corrosion rate, CR for UT, LT and PDMS-LT.

The application of PDMS coating on the laser-textured surfaces (PDMS-LT) further decreases the corrosion rates (Guan et al., 2021). The PDMS-LT surface exhibits the lowest corrosion rate at 52.89 mpy, demonstrating the effectiveness of the hydrophobic PDMS layer in protecting against corrosive environments. Similarly, the PDMS-LT surfaces show significantly reduced 84% corrosion rates, compared to UT surface.

As shown by the Tafel plot in Figure 15, the most noteworthy result of this work is that the combination of laser texturing and PDMS coating significantly improves the corrosion resistance of Ti6Al4V surfaces. The PDMS coating offers further protection because of its hydrophobic qualities, while the laser texturing process lowers the corrosion rate by producing a more stable and passive surface. These findings highlight the significance of surface changes in enhancing titanium alloy performance and endurance in corrosive conditions. Combining PDMS coating with laser texturing presents a viable way to increase the dependability and longevity of Ti6Al4V components in a range of industrial applications.

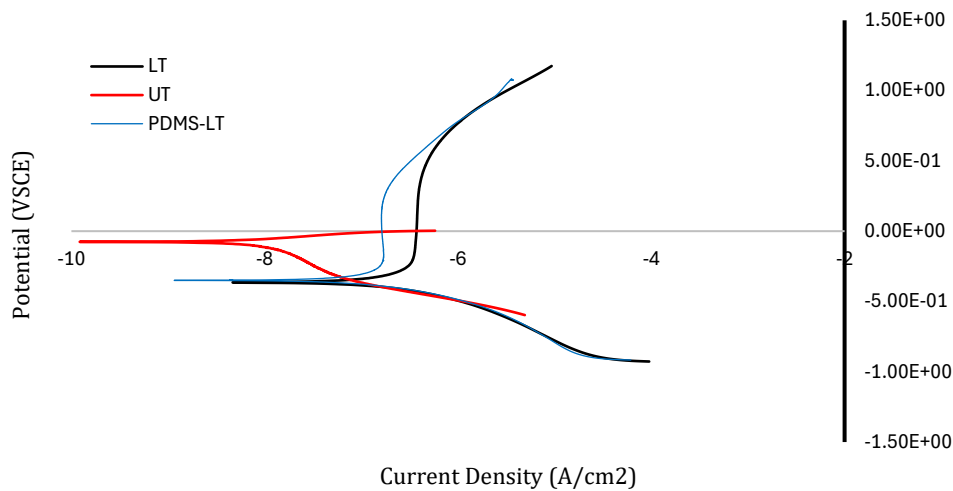


Figure 15: Tafel plot for untextured (UT), laser textured (LT) and laser textured prior to PDMS coating (PDMS-LT).

In summary, the corrosion rate analysis demonstrates that laser texturing combined with PDMS coating significantly improves the corrosion resistance of Ti6Al4V surfaces. This study underscores the importance of coating and surface modification by laser texturing to enhance the durability and performance of titanium alloys in corrosive environments.

## CONCLUSIONS

This study investigates the effects of laser texturing and PDMS coating on the wear and corrosion resistance of Ti6Al4V surfaces.

- a. In dry conditions, UT and LT surfaces had identical wear rates, indicating laser texturing alone does not significantly alter wear performance. However, the PDMS-LT surface showed a 29.41% reduction in wear rate compared to UT, demonstrating the PDMS coating's effectiveness in reducing wear.



- b. All surfaces showed lower wear rates under seawater lubrication than in dry conditions. The UT surface exhibited a 54% lower wear rate, and the LT surface showed further reduction, highlighting laser texturing's positive impact. The PDMS-LT surface maintained low wear rates, slightly higher than LT, indicating the PDMS coating's partial influence in seawater.
- c. The most significant wear rate reduction occurred under oil lubrication. The UT surface showed a slight improvement, while the LT surface had a greater reduction in wear rate. The PDMS-LT surface exhibited the lowest wear rate at  $2.83 \times 10^{-4} \text{ mm}^3/\text{m.N}$ , with an 80% improvement over UT, demonstrating the synergistic effect of PDMS coating and oil lubrication.
- d. The PDMS coating on LT surfaces significantly decreased corrosion rates. The PDMS-LT surface in the grid pattern exhibited the lowest corrosion rate at  $5.30 \times 10^{-4} \text{ mpy}$ , demonstrating the hydrophobic PDMS layer's effectiveness in protecting against corrosion.

#### ACKNOWLEDGEMENT

Ministry of Higher Education for the financial support under FRGS/1/2020/TK0/USM/02/37 (203.PMEKANIK.6071486) and Universiti Malaysia Pahang Flagship Grant (PDU213002-1).

#### REFERENCES

- Alsaigh, R. A. (2024). Enhancement of Surface Properties Using Ultrashort-Pulsed-Laser Texturing: A Review. *Crystals*, 14(4). <https://doi.org/10.3390/cryst14040353>
- Chauhan, A. S., Jha, J. S., Telrandhe, S., V. S., Gokhale, A. A., & Mishra, S. K. (2021). Laser surface treatment of  $\alpha$ - $\beta$  titanium alloy to develop a  $\beta$  -rich phase with very high hardness. In *Journal of Materials Processing Technology* (Vol. 288). <https://doi.org/10.1016/j.jmatprotec.2020.116873>
- Cholkar, A., Mccann, R., Perumal, G., & Chatterjee, S. (2023). Applied Surface Science Advances Advances in laser-based surface texturing for developing antifouling surfaces: A comprehensive review. *Applied Surface Science Advances*, 18(November), 100513. <https://doi.org/10.1016/j.apsadv.2023.100513>
- Davaasuren, G., Ngo, C. V., Oh, H. S., & Chun, D. M. (2014). Geometric study of transparent superhydrophobic surfaces of molded and grid patterned polydimethylsiloxane (PDMS). *Applied Surface Science*, 314, 530–536. <https://doi.org/10.1016/j.apsusc.2014.06.170>
- Farrokhi, H., Zhou, W., & Zheng, H. (2015). Theoretical analysis of non-ablative laser texturing of silicon surface with a continuous wave fiber laser. *Journal of Laser Micro Nanoengineering*, 10(2), 181–185. <https://doi.org/10.2961/jlmn.2015.02.0014>
- Guan, J., Jiang, X., Xiang, Q., Yang, F., & Liu, J. (2021). Corrosion and tribocorrosion behavior of titanium surfaces designed by electromagnetic induction nitriding for biomedical applications. *Surface and Coatings Technology*, 409(116). <https://doi.org/10.1016/j.surfcoat.2021.126844>
- Guo, Y., & Zhao, H. (2024). Femtosecond laser processed superhydrophobic surface. *Journal of Manufacturing Processes*, 109(August 2023), 250–287. <https://doi.org/10.1016/j.jmapro.2023.12.005>
- Harun, D., Mohd Tobi, A. L., & Jamian, S. (2020). Investigation on the effect of reciprocating sliding wear test for titanium alloy, Ti-6Al-4V under frequency set up. *International Journal of*

- Emerging Trends in Engineering Research, 8(1 Special Issue 2), 23–28. <https://doi.org/10.30534/ijeter/2020/0481.22020>
- He, H., Hua, R., Li, X., Wang, C., Ning, X., & Sun, L. (2020). Fabrication of superhydrophobic Ti-6Al-4V surfaces with single-scale micotextures by using two-step laser irradiation and silanization. *Materials*, 13(17). <https://doi.org/10.3390/ma13173816>
- He, H., Wu, W., Xi, Z., Ma, Z., Zhang, L., Wang, C., & Sun, L. (2022). Time dependency of superhydrophilic and superhydrophobic surfaces produced by nanosecond laser irradiation assisted by post-annealing and silanization. *Applied Surface Science*, 586(February). <https://doi.org/10.1016/j.apsusc.2022.152819>
- Hu, J., & Xu, H. (2016). Friction and wear behavior analysis of the stainless steel surface fabricated by laser texturing underwater. *Tribology International*, 102, 371–377. <https://doi.org/10.1016/j.triboint.2016.06.001>
- Hu, L., Zhang, L., Wang, D., Lin, X., & Chen, Y. (2018). Fabrication of biomimetic superhydrophobic surface based on nanosecond laser-treated titanium alloy surface and organic polysilazane composite coating. *Colloids and Surfaces A: Physicochemical and Engineering Aspects*, 555(May), 515–524. <https://doi.org/10.1016/j.colsurfa.2018.07.029>
- Huerta-Murillo, D., García-Girón, A., Romano, J. M., Cardoso, J. T., Cordovilla, F., Walker, M., Dimov, S. S., & Ocaña, J. L. (2019). Wettability modification of laser-fabricated hierarchical surface structures in Ti-6Al-4V titanium alloy. *Applied Surface Science*, 463(September 2018), 838–846. <https://doi.org/10.1016/j.apsusc.2018.09.012>
- Kameya, Y. (2017). Wettability modification of polydimethylsiloxane surface by fabricating micropillar and microhole arrays. *Materials Letters*, 196. <https://doi.org/10.1016/j.matlet.2017.03.103>
- Khatri, N., Barkachary, B. M., Singh, S., Manjunath, K., Chandra, N., Armstrong, J., Agrawal, A., & Goel, S. (2024). Diamond machining of additively manufactured Ti6Al4V ELI : Newer mode of material removal challenging the current simulation tools. *Journal of Manufacturing Processes*, 120(April), 378–390. <https://doi.org/10.1016/j.jmapro.2024.04.051>
- Kumar, A., & Singh, G. (2024). Surface modification of Ti6Al4V alloy via advanced coatings: Mechanical, tribological, corrosion, wetting, and biocompatibility studies. *Journal of Alloys and Compounds*, 989(April), 174418. <https://doi.org/10.1016/j.jallcom.2024.174418>
- Lei, X., Lin, N., Yuan, S., Lei, C., Nouri, M., Liu, Z., Yu, Y., Zeng, Q., Ma, G., Li, D., & Wu, Y. (2024). Combining laser surface texturing and double glow plasma surface chromizing to improve tribological performance of Ti6Al4V alloy. *Surface and Coatings Technology*, 478(August 2023), 130418. <https://doi.org/10.1016/j.surfcoat.2024.130418>
- Madapana, D., Bathe, R., Manna, I., & Majumdar, J. D. (2024). Effect of process parameters on the corrosion kinetics and mechanism of nanosecond laser surface structured titanium alloy (Ti6Al4V). *Applied Surface Science Advances*, 20(February), 100580. <https://doi.org/10.1016/j.apsadv.2024.100580>
- Nazrin, A., Ismail, N., Tomadi, S. H., Farah, N., Abd, H., & Ayu, M. (2024). Effect of dry and MQL cutting condition on coated carbide cutting tool during the end milling of Ti-6Al-4V titanium alloy. *Jurnal Tribologi*, 41(March), 162–176.
- Olkowicz, K., Buczko, Z., Nasiłowska, B., Kowalczyk, K., & Czwartos, J. (2022). Superhydrophobic Coating Based on Porous Aluminum Oxide Modified by Polydimethylsiloxane (PDMS). *Materials*, 15(3), 1–15. <https://doi.org/10.3390/ma15031042>
- Parmar, V., Kumar, A., Mani Sankar, M., Datta, S., Vijaya Prakash, G., Mohanty, S., & Kalyanasundaram, D. (2018). Oxidation facilitated antimicrobial ability of laser micro-textured

- titanium alloy against gram-positive *Staphylococcus aureus* for biomedical applications. *Journal of Laser Applications*, 30(3), 032001. <https://doi.org/10.2351/1.5039860>
- Rasitha, T. P., Krishna, N. G., Anandkumar, B., Vanithakumari, S. C., & Philip, J. (2024). A comprehensive review on anticorrosive/antifouling superhydrophobic coatings: Fabrication, assessment, applications, challenges and future perspectives. *Advances in Colloid and Interface Science*, 324(January), 103090. <https://doi.org/10.1016/j.cis.2024.103090>
- Schnell, G., Polley, C., Bartling, S., & Seitz, H. (2020). Effect of chemical solvents on the wetting behavior over time of femtosecond laser structured Ti6Al4V surfaces. *Nanomaterials*, 10(6), 1–20. <https://doi.org/10.3390/NANO10061241>
- Sulym, I., Goncharuk, O., Storozhuk, L., Terpiłowski, K., Sternik, D., Pakhlov, E., Diahm, S., & Valdez-Nava, Z. (2024). Development of MWCNTs@PDMS nanocomposites with enhanced hydrophobicity and thermo-oxidative stability. *Applied Surface Science*, 667(May). <https://doi.org/10.1016/j.apsusc.2024.160405>
- Tan, N., Li, Y., Lou, L. yan, Zhang, G. liang, Xing, Z. guo, & Wang, H. dou. (2021). Influence of micro-nano multiscale surface texture on wettability of Ni-based droplets at high temperature. *Surface and Coatings Technology*, 418(January), 127103. <https://doi.org/10.1016/j.surfcoat.2021.127103>
- Trinh, K. E., Ramos-Moore, E., Green, I., Pauly, C., Zamanzade, M., & Mucklich, F. (2017). Topographical and Microstructural Effects of Laser Surface Texturing on Tin-Coated Copper Electrical Connectors under Load Cycling. *IEEE Transactions on Components, Packaging and Manufacturing Technology*, 7(4), 582–590. <https://doi.org/10.1109/TCPMT.2017.2659224>
- Velayuthaperumal, S., & Radhakrishnan, R. (2024). A novel nanosecond pulsed laser textured moat configurations for enhancing surface wettability, corrosion and tribology behaviour of Ti6Al4V implant material. *Materials Today Communications*, 39(February), 108701. <https://doi.org/10.1016/j.mtcomm.2024.108701>
- Wang, Y., Zhao, X., Ke, C., Yu, J., & Wang, R. (2020). Nanosecond laser fabrication of superhydrophobic Ti6Al4V surfaces assisted with different liquids. *Colloids and Interface Science Communications*, 35(March), 100256. <https://doi.org/10.1016/j.colcom.2020.100256>
- Wang, Z., He, H., Wu, S., Xiang, J., & Ni, J. (2022). Effect of surface topography and wettability on friction properties of CFRPEEK. *Tribology International*, 171(March), 107573. <https://doi.org/10.1016/j.triboint.2022.107573>
- Xu, Q., Chen, L., Sun, M., Wang, G., & Liu, Y. (2021). A comparative study of corrosion property, tribological behavior and cutting performance of tool materials for the cutting of marine high-strength steels in the marine environment. *Proceedings of the Institution of Mechanical Engineers, Part B: Journal of Engineering Manufacture*, 235(1–2), 98–111. <https://doi.org/10.1177/0954405420949225>
- Yang, H., Zheng, H., & Zhang, T. (2024). Tribology International A review of artificial intelligent methods for machined surface roughness prediction. *Tribology International*, 199(June), 109935. <https://doi.org/10.1016/j.triboint.2024.109935>
- Yang, Z., Zhu, C., Zheng, N., Le, D., & Zhou, J. (2018). Superhydrophobic surface preparation and wettability transition of titanium alloy with micro/nano hierarchical texture. *Materials*, 11(11), 1–15. <https://doi.org/10.3390/ma11112210>
- Yusuf, Y., Ghazali, M. J., Abdollah, M. F. Bin, dan Pembuatan, F. T. K. M., Malaysia, U. T., & Tunggal, D. (2022). Self-cleaning plasma sprayed TiO<sub>2</sub> coatings modified by laser surface texturing process. *Jurnal Tribologi*, 34, 39–55.

- Zhu, T., Cheng, Y., Huang, J., Xiong, J., Ge, M., Mao, J., Liu, Z., Dong, X., Chen, Z., & Lai, Y. (2020). A transparent superhydrophobic coating with mechanochemical robustness for anti-icing, photocatalysis and self-cleaning. *Chemical Engineering Journal*, 399(March), 125746. <https://doi.org/10.1016/j.cej.2020.125746>
- Zul, M. H., Ishak, M., Aiman, M. H., & Quazi, M. M. (2023). Fabrication of Superhydrophobic on Ti6Al4V by Using the Hybrid Process of Nanosecond Laser Texturing BT - Proceedings of the 2nd Energy Security and Chemical Engineering Congress (N. H. Johari, W. A. Wan Hamzah, M. F. Ghazali, H. D. Setiabudi, & S. Kumarasamy, Eds.; pp. 341–350). Springer Nature Singapore.